Cell. Mol. Life Sci. 63 (2006) 2405–2414
1420-682X/06/202405-10
DOI 10.1007/s00018-006-6248-7

Cellular and Molecular Life Sciences

Research Article

Specific cleavage of insulin-like growth factor-binding protein-1 by a novel protease activity

J. Wang [a], J. Shafqat [b], K. Hall [a], M. Ståhlberg [b], I.-L. Wivall-Helleryd [a], K. Bouzakri [a], J. R. Zierath [a], K. Brismar [a], H. Jörnvall [b] and M. S. Lewitt [a, *]

[a] Department of Molecular Medicine and Surgery, L1:01, Karolinska Institutet and Hospital Solna, 171 76 Stockholm (Sweden), Fax: +46 8 51776900, e-mail: Moira.Lewitt@ki.se
[b] Medical Biochemistry and Biophysics, Karolinska Institutet, 171 77 Stockholm (Sweden)

Received 26 May 2006; received after revision 21 June 2006; accepted 24 August 2006
Online First 28 September 2006

Abstract. Insulin-like growth factor-binding protein-1 (IGFBP-1) is secreted in a highly phosphorylated form that binds IGF-I with high affinity and is resistant to proteolysis. We have purified IGFBP-1-specific protease activity from the urine of an individual with multiple myeloma. This protease efficiently cleaves both phosphorylated and non-phosphorylated IGFBP-1 at Ile^{130}-Ser^{131}, generating fragments that together have higher association and dissociation rates for IGFs compared with intact IGFBP-1. The proteolytic fraction contained azurocidin, a protease homologue hitherto considered inactive. After cleavage of IGFBP-1, there was a lower affinity, but higher capacity for IGF-I binding, suggesting both N- and C-terminal fragments may interact with ligand independently. There was decreased inhibition of IGF-II-stimulated cell growth and glucose uptake. Alone, proteolysed IGFBP-1 stimulated glucose uptake in muscle. We conclude that specific cleavage of IGFBP-1 at target tissues is important in cellular growth and metabolism and opens novel strategies for targeting IGFBP-1 in treatment of disease.

Keywords. Insulin-like growth factor, IGF-binding protein-1, proteolysis, skeletal muscle, catabolism, azurocidin/heparin binding protein/CAP37.

Introduction

The insulin-like growth factor-binding proteins (IGFBPs) are a family of six homologous proteins with multifunctional roles through interactions with IGFs and other proteins [1]. These actions are modified by posttranslational modifications, such as phosphorylation and proteolysis. IGFBP-1 plays an endocrine role in nutrition [2]. The major circulating isoform is secreted by the liver, and is highly phosphorylated and has higher IGF-I binding affinity than lesser phosphorylated forms [3, 4]. Hepatic IGFBP-1 is transcriptionally inhibited by insulin, and stimulated by cytokines, glucocorticoids, and cAMP- and AMPK-dependent pathways [5–7]. There is a diurnal variation in circulating IGFBP-1 levels, which inhibit the availability of IGFs to stimulate anabolism, including glucose uptake [2, 7]. High circulating levels in catabolic states are resistant to inhibition by insulin [8], predict poor survival [8, 9], and may contribute to wasting in catabolism through inhibition of IGF-mediated protein synthesis [10].

Originally purified from amniotic fluid [11], a paracrine role of IGFBP-1 involves dephosphorylation by placental phosphatases, which is reported to make it susceptible to proteolysis [12, 13]. The regulation of endocrine IGFBP-1 activity at the level of its target tissues is little studied. This is potentially a very important level of regulation, and targeting IGFBP-1 for degradation could be of benefit in conditions of catabolism or hepatic insulin resistance. Conversely, reducing IGFBP-1 degradation is expected

* Corresponding author.

to be useful in conditions where IGFs have a pathogenic role, such as in malignancy [14] and vascular disease [15]. It is possible that cleavage of IGFBP-1 would result in increased IGF availability and in preserved effects on cell migration through interaction of its Arg-Gly-Asp (RGD) sequence with the $\alpha5\beta1$ integrin [16]. Previously it has been suggested that proteolysis of IGFBP-4 by PAPP-A increases local IGF action and in this way contributes to neointimal hyperplasia [17].

Here we describe a protease that specifically cleaves IGFBP-1 to generate IGF-binding fragments with lower IGF affinity. It is a potential target in strategies to modify IGF actions.

Material and methods

Materials. All peptides used were human isoforms. Recombinant IGF-I, nonphosphorylated (np) IGFBP-1 and phosphorylated (p) IGFBP-1 were gifts from Kabi Pharmacia (Sweden), and IGF-II was donated by Eli Lilly (Indianapolis, IN). IGF-I was iodinated using lactoperoxidase and purified by HPLC. npIGFBP-1 was iodinated by the chloramine T method, purified on a PD10-G25 column (Amersham Biosciences UK) and used within 5 days. npIGFBP-1 and pIGFBP-1 were biotinylated with sulfo-NHS-LC-LC-biotin (EZ-Link, Pierce) according to the product instructions. Highly phosphorylated HepG2-purified IGFBP-1 and a dephosphorylated preparation from the same source were purchased from Sigma-Aldrich (Sweden). IGFBP-2, glycosylated IGFBP-3, IGFBP-4, IGFBP-6 and des-IGF-I were from GroPep Limited (Adelaide, Australia), and IGFBP-5 from Upstate (KELAB, Göteborg, Sweden). Recombinant human azurocidin$^{27–250}$ and a monoclonal antibody to human azurocidin were obtained from R&D Systems (Abingdon, UK) and a monoclonal antibody to human mast cell chymase, from Calbiochem (Darmstadt, Germany). Other reagents were from Sigma-Aldrich, unless otherwise indicated.

Protease assays. Proteolysis was carried out in phosphate-buffered saline (PBS), pH 7 (Invitrogen) at 37 °C for 2 h, unless otherwise indicated. When using pure IGFBPs as substrates, equimolar concentrations of each were incubated without and with urine, followed by affinity labeling with [^{125}I]IGF-I using disuccinimidyl suberate (DSS) (Pierce, Rockford, IL) and separation on 14% nonreducing SDS-PAGE. Gels were fixed, dried and analyzed with the Fuji PhosphoImage program (Fuji Co., Stockholm, Sweden). When iodinated IGFBP-1 was used as substrate, fragments were separated from the intact form on 12% SDS-PAGE under nonreducing conditions and autoradiographed as described above. Biotinylated IGFBP-1 and its proteolytic fragments were separated on 12% or 14% SDS-PAGE under reducing conditions, transferred to PVDF membrane (Bio-Rad, Sundbyberg, Sweden), incubated with 1:5000 neutravidin-horseradish peroxidase (Pierce) at 22 °C for 60 min and detected by ECL (Amersham Biosciences, Uppsala, Sweden). In a plate assay, biotinylated IGFBP-1 was bound to streptavidin-coated plates (Delfia, Perkin-Elmer, Boston, MA), and then incubated without and with protease in PBS, pH 7 at 37 °C for 5 h. After washing, IGF-binding fragments were determined by incubation with radioiodinated IGF-I for 2 h at 22 °C. Unbound tracer was removed by washing, and the bound portion of tracer was removed by acidification and the counts determined in a gamma counter. Silver staining of pure proteins was performed after 12% SDS-PAGE gel under reducing conditions with the SilverQuest kit (Invitrogen, Stockholm, Sweden). Cleavage of synthetic succinyl-WDAISYD-*p*-nitroanilide (Cambridge Peptides, Suffolk, UK) was analyzed by MALDI-MS.

Purification of azurocidin from human urine. Human urine was collected with approval of the local Ethics Committee. Heparin affinity chromatography was carried out in batches using heparin-agarose gel (Amersham Biosciences, UK). Urine was diluted 1:5 in 10 mM sodium phosphate, with 0.25 M NaCl, pH 7, and incubated with gel for 30 min on ice with continuous stirring. After washing the gel with 10 volumes of loading buffer, the salt content was increased to 2 M NaCl. The eluate was desalted (to approx 0.2 M NaCl), concentrated using a 10-kDa cut-off Microsep™ spin column (PALL Life Sciences, USA), and stored at –80 °C. Concentrated material derived from a 700-ml urine sample was applied to C4 reverse-phase HPLC, in 0.1% TFA on an acetonitrile gradient of 0–100%. Immunoaffinity chromatography was carried out by attaching monoclonal antibodies to protein G Sepharose (Sigma-Aldrich, Sweden). The antibody-bound gel was incubated with the eluate from heparin affinity chromatography for 2 h at 22 °C, and transferred to a Bio-Spin chromatography column (Bio-Rad). The flow-through was collected for analysis.

Sequence analysis. The cleavage sites in IGFBP-1 were determined by HPLC-separation of the fragments after incubation with the heparin affinity eluate, followed by N- and C-terminal sequence degradations in ABI instruments as described [18]. Nu-PAGE (Invitrogen) was used to separate proteins in samples that would be subjected to in-gel digestion with trypsin for LC-MS/MS and MALDI MS analysis [19]. The azurocidin quantity in the urine, estimated from sequencer analysis, was 25 pmol/100 ml.

Biacore analysis. Instrument and reagents (buffers, chemicals for activating and deactivating) were purchased from Biacore (Uppsala, Sweden). IGF-I, IGF-II and des(1–3)IGF-I were immobilized on the sensor chip by amine coupling and deactivated with 0.1 M ethanol-

amine. A reference flow cell was also prepared to correct for background and bulk refractive index contribution. After adding equilibration buffer to achieve a stable baseline, binding experiments were performed at 22 °C with the samples injected in random order. From each sample, 40 µl was injected over the sensor surface at a rate of 10 µl/min (association period), followed by a 6-min wash with buffer (dissociation period). The sensor surface was regenerated with 20 µl 100 mM HCl and washed for 6 min before the next sample. We used a 1:1 Langmuir binding interaction model for kinetic analysis using the Biacore software and GraphPad Prism (GraphPad Software Inc, San Diego, CA).

Cell studies. MCF-7 human breast cancer cells were maintained in MEM alpha ribonucleic acid-free medium supplemented with 10% fetal bovine serum, 50 U/ml penicillin sodium, 50 µg/ml streptomycin sulfate and 2 mM L-glutamine at 37 °C in 5% CO_2 humidified environment. Human skeletal muscle cells were isolated, with approval from the local Ethics Committee, from the muscle biopsy specimens by trypsin digestion, and were grown to confluent myoblasts and differentiated into myotubes as previously described in detail [20]. Muscle from four different subjects were individually minced before being incubated for 30 min in 5 ml trypsin-EDTA (Invitrogen, Carlsbad, CA) at 37 °C under agitation. After being centrifuged (150 *g*), the pellet was rinsed several times in PBS. Cells were first preplated for 1 h to eliminate rapidly adherent fibroblasts. The remaining cells were then cultured in a growth medium composed of HAM F-10 supplemented with 20% fetal bovine serum (FBS; Invitrogen, Stockholm, Sweden), and 1% antibiotics (Invitrogen, Sweden). Cells were plated in 6-well plates and cultured in growth medium at 37 °C until confluence. Differentiation into myotubes was induced by changing the medium to Dulbecco's modified Eagle's medium supplemented with 2% FBS, and 1% antibiotics. Cells showed polynucleated status and expressed specific markers of human skeletal muscle 4 days after differentiation was initiated [20].

[^{3}H]Thymidine incorporation. Experiments were carried out in 48-well plates, at 70% confluence. After a 20-h incubation in serum-free medium supplemented with 0.1% BSA, the experimental conditions were added for a further 24 h, with [^{3}H]thymidine (1 µCi/ml) added for the last 4 h. Cells were then washed with ice-cold 0.9% NaCl three times and incubated with ice-cold 5% TCA for 15 min at 22 °C. The fixed nucleotides were solubilized in 0.1 M NaOH at 22 °C and subjected to liquid scintillation counting.

2-Deoxyglucose transport. Glucose uptake was performed as previously described for primary human muscle cells [21]. After 24-h serum starvation, myotubes were pre-incubated with or without IGF-II (10 ng/ml) and IGF-II + IGFBP-1 (intact or cleaved at 20 or 80 ng/ml) for 90 min. IGF-II and IGFBP-1 were mixed 30 min before the experiments. Cells were then washed four times with pre-warmed buffer (150 mM NaCl, 5 mM KCl, 1.2 mM $MgSO_4$, 1.2 mM $CaCl_2$, 2.5 mM NaH_2PO_4, 10 mM HEPES, pH 7.4) and glucose uptake was measured for 15 min using [^{3}H]2-deoxyglucose (50 µM, 14 800 Bq/well). Results were expressed as the percentage of glucose uptake in the absence of IGF-II or IGFBP-1.

Statistical analyses. The effect of divalent cations on the degree of IGFBP-1 proteolysis was determined by *t*-test. The Biacore kinetic analysis was by one-way ANOVA. The effect of IGF-II and IGFBP-1 in muscle cell culture was analyzed by two-way ANOVA. Where significant differences were observed, comparisons were made using the Tukey test. In the study using MCF-7 breast cancer cells the Wilcoxon Matched Pairs test was used. Statistical significance was set at $p < 0.05$.

Results

Discovery of a specific IGFBP-1 protease in human urine. In screenings of human urine for IGFBP-1 protease activity, we found one individual with a specific IGFBP-1 protease. This 73-year old woman had a long history of atopy with inflammatory skin lesions and eosinophilia, and a 7-year history of monoclonal gammopathy. Over the next 3 years this progressed to a smouldering myeloma. Urine from this individual cleaved native IGFBP-1, both the highly phosphorylated and the dephosphorylated isoforms (Fig. 1). After a 2-h incubation at 37 °C, pH 7, 1 µl urine cleaved more than 50% of 10 ng of each IGFBP-1 isoform, while 2 µl had minimal effect on the same amount of IGFBP-2, glycosylated IGFBP-3 and,

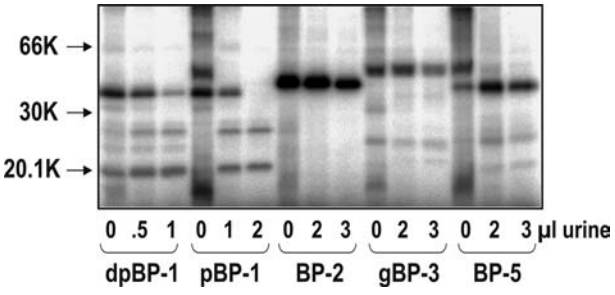

Figure 1. IGFBP-1-specific protease activity in human urine. Pure IGFBPs, 10 ng, were incubated with the indicated volumes of urine at pH 7 for 2 h at 37 °C. No IGF or IGFBP immunoreactivity was detectable in the urine. After incubation, dephosphorylated (dp) and phosphorylated (p)IGFBP-1, IGFBP-2, glycosylated (g) IGFBP-3 and IGFBP-5, were cross-linked to radioiodinated IGF-I and subjected to 14% SDS-PAGE. The gel was dried and autoradiographed. Molecular mass markers are indicated by the arrows.

not shown, IGFBP-4 and IGFBP-6. For IGFBP-5, there was a loss of the ~50-kDa form and an increase in the 40-kDa form after exposure to 2 µl urine. This may represent limited proteolysis, but there was no further degradation at a higher concentration of urine. This urinary IGFBP-1 protease activity was inhibited by PMSF (10 mM), chymostatin (10 µM), and the kallikrein inhibitor cyclohexylacetyl-Phe-Arg-Ser-Val-Gln (100 µM) (Fig. 2a). Aprotinin was not inhibitory and in this experiment promoted protease activity slightly. Not shown here, TPCK (1 mM) inhibited proteolysis, while TLCK did not. Proteolysis was inhibited by divalent metal cations, such as $CuCl_2$, $NiCl_2$, and $CoCl_2$, while $CaCl_2$ had a significant promoting effect on activity (Fig. 2b). EDTA, EGTA and 1,10-phenanthroline had no effect on the efficiency of IGFBP-1 degradation (data not shown). In addition to the proteolytic activity at pH 7–8, the urine contained activity at pH 2–4 (Fig. 3a), which was inhibited by pepstatin A (Fig. 3b). There was a complete loss of IGFBP-1 protease activity at pH 2 when acid-activated urine was neutralized, and re-acidified (Fig. 3c), a process known to destroy pepsin [22].

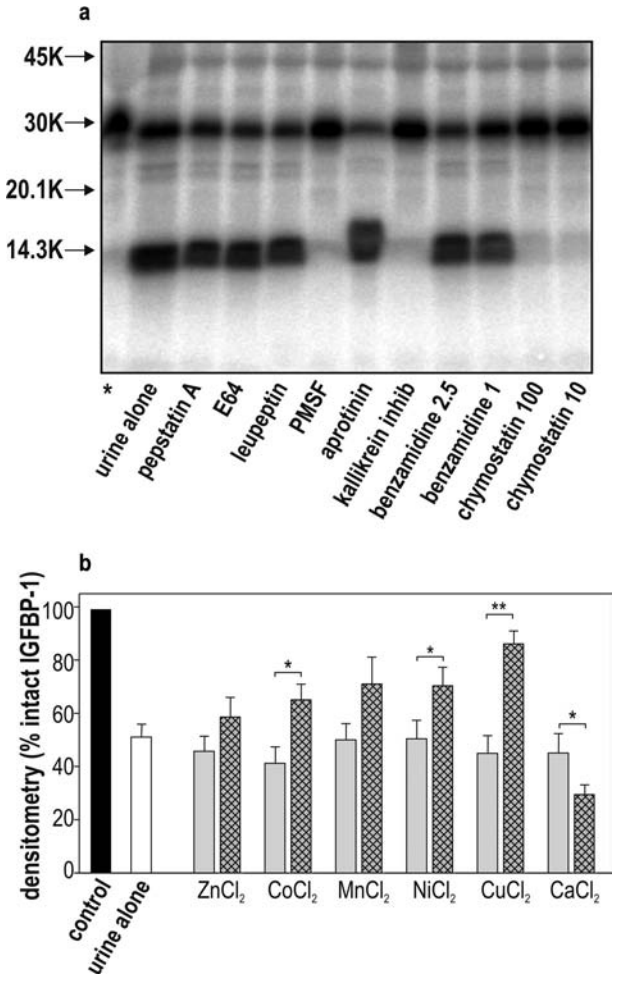

Figure 2. Effect of protease inhibitors and divalent cations on urinary protease activity at neutral pH. Radioiodinated recombinant npIGFBP-1 was incubated alone (*) or in the presence of 0.5 µl urine, in the absence and presence of protease inhibitors or metal cations at pH 7 for 2 h at 37 °C, then subjected to 14% SDS-PAGE and the fragments detected by autoradiography. (*a*) Effect of 100 µM pepstatin A, 10 µM E64, 2.5 mM leupeptin, 10 mM PMSF, 100 µM aprotinin, 2.5 mM kallikrein inhibitor and benzamidine (mM) and chymostatin (µM). Molecular mass markers are indicated by the arrows. (*b*) Densitometry measurements of intact IGFBP-1. The results are the mean ± SEM, pooled from six to eight experiments. The effects of 10 mM of each cation are displayed in the hatched bars alongside the effect of urine in the absence of cation (light gray bars). The mean effect of urine from all the experiments is shown in the open bar. * $p < 0.05$; ** $p < 0.01$ (paired *t*-test).

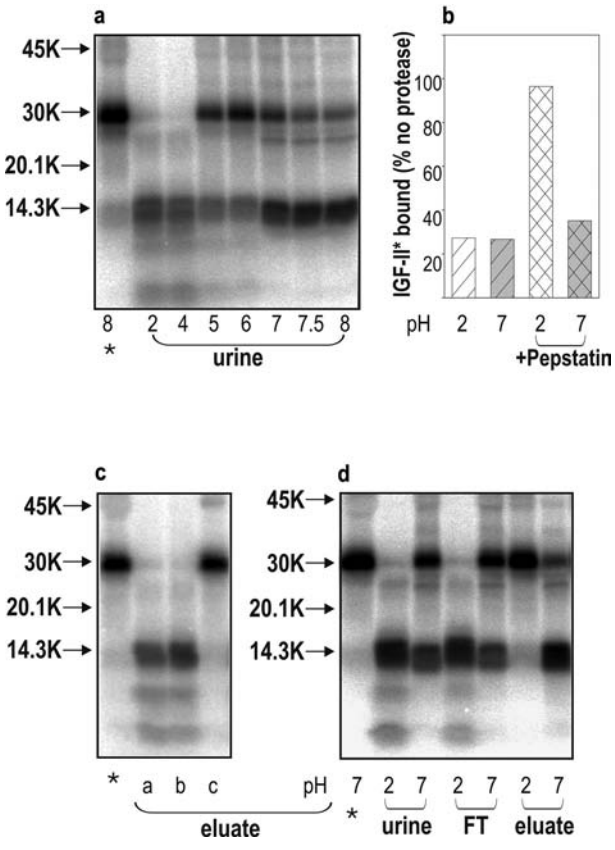

Figure 3. Separation of acid-activated and neutral IGFBP-1 protease activity in human urine. (*a*) pH dependence of urinary IGFBP-1 protease activity. Radioiodinated recombinant npIGFBP-1 was subjected to 14% SDS-PAGE alone (*) or after proteolysis with 0.5 µl urine for 2 h at 37 °C at the pH indicated and the fragments detected by autoradiography. Molecular mass markers are indicated by the arrows. (*b*) Biotinylated recombinant npIGFBP-1 (10 ng) was bound to streptavidin coated plates and incubated with 5 µl urine for 2 h at 37 °C in the presence and absence of 10 µM pepstatin A at pH 2 and 7. The wells were washed, incubated with radioiodinated IGF-II for 2 h at 22 °C, washed, and the bound counts detected. (*c*) Acid-activated protease activity is destroyed by neutralization. Radioiodinated pIGFBP-1 was incubated without (*) and with 0.5 µl urine for 2 h at 37 °C at pH 2. Prior to incubation the urine was either untreated (lane a), adjusted to pH 2 for 15 min (lane b) or adjusted to pH 2 for 15 min and then to pH 7 for a further 15 min (lane c). (*d*) Effect of urine, 0.5 µl, flow-through (FT 0.5 µl) from the heparin affinity column, and eluate (derived from 25 µl urine) on cleavage of radioiodinated pIGFBP-1 at pH 2 and 7.

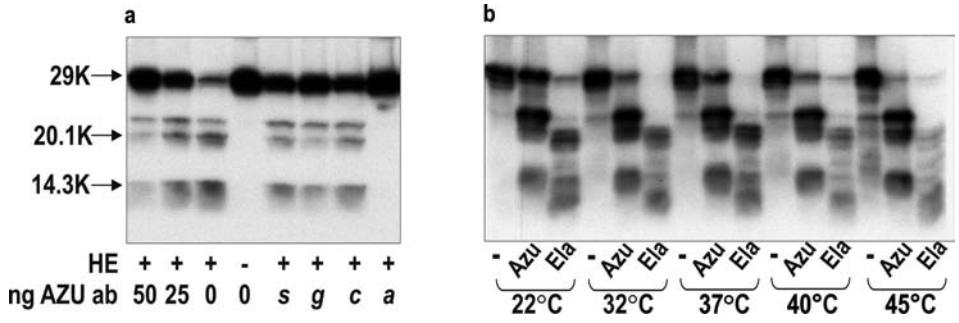

Figure 4. Azurocidin-dependent IGFBP-1 protease activity. Biotinylated recombinant phosphorylated IGFBP-1 was incubated at pH 7 for 2 h. Fragments were separated on SDS-PAGE, and detected by ECL, as described in the Methods. (*a*) Incubations at 37 °C with 0.25 µL eluate from heparin affinity purification of 25 µl urine (HE) in the presence and absence of anti-azurocidin antibody (AZU ab), alongside incubation with 1 µl of the starting material from a different affinity purification (s), and the flow-through from protein G columns without (g) and with bound anti-chymase (c) or anti-azurocidin (a) antibodies. (*b*) Incubations without (-) and with heparin affinity purified urine containing 63 fmol azurocidin (Azu), or with 63 fmol elastase (Ela) at increasing temperatures.

The neutral protease activity, but not the acid-activated protease, bound to a heparin affinity column and was eluted in 2 M NaCl (Fig. 3d). The effect of protease inhibitors and divalent ions on the activity of the heparin affinity eluate was the same as their effect on the original urine (data not shown). Silver staining of the heparin affinity eluate after gel electrophoresis revealed three proteins, identified by mass spectrometry as azurocidin[27–251] (heparin-binding protein/CAP37), myeloperoxidase and lactoferrin. The proteolytic effect of the heparin affinity eluate on IGFBP-1 was completely abolished in the presence of a monoclonal antibody to azurocidin (Fig. 4a). Furthermore, using this antibody for immunoaffinity chromatography, specific extraction of azurocidin resulted in complete loss of proteolytic activity (Fig. 4a).

Cleavage of IGFBP-1 at a unique site. Proteolysis of pIGFBP-1 was seen within minutes, using an azurocidin: substrate molar ratio of 1:3500 (Fig. 5). When unlabeled IGFBP-1 was cleaved and detected by silver staining after SDS-PAGE, the major fragments migrated at 20 and 14 kDa (Figs 5 and 6a). When these bands were excised and the tryptic digests analyzed by MALDI-MS, both bands contained sequences corresponding to the N- and C-terminal regions of IGFBP-1 (Fig. 6b). Consistent with this, fragments migrating at 22, 20 and 14 kDa were seen after proteolysis when IGFBP-1, biotinylated at the N terminus, was used as substrate (Fig. 4a).

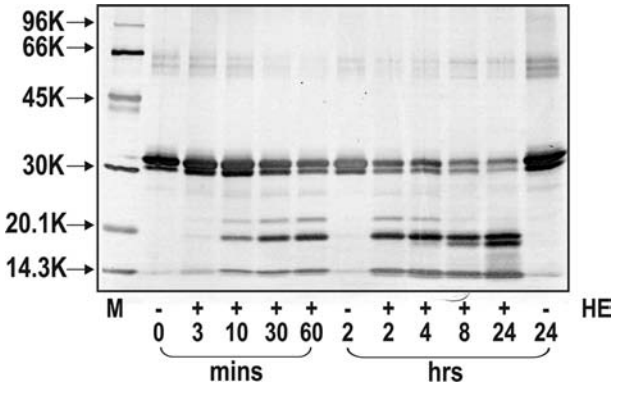

Figure 5. Phosphorylated IGFBP-1 is efficiently cleaved. Recombinant IGFBP-1 was incubated with the eluate from heparin affinity purification of urine (HE) with a ratio of azurocidin:IGFBP-1 of 1:3500. After the times indicated, proteins were detected by silver staining after SDS-PAGE.

Proteolysed recombinant npIGFBP-1 was subjected to HPLC and peaks were sequenced and visualized on SDS-PAGE. Shown in Figure 6a, fragments containing the N-terminal region of IGFBP-1 migrated at 20 kDa, while C-terminal fragments migrated at 14 kDa. Similar results were obtained for recombinant pIGFBP-1 (data not shown). There were four HPLC runs, two using recombinant npIGFBP-1 and two using recombinant pIGFBP-1 and the results are summarized in Figure 6b. The primary cleavage site, identified by N-terminal sequencing in all four runs, was at Ile[130]-Ser[131] and was confirmed by C-terminal sequence analysis on one of the runs. Cleavage after isoleucine was also observed using a synthetic substrate Trp-Asp-Ala-Ile-Ser-Thr-Tyr-Asp (IGFBP-1[127–134]). A secondary cleavage site, present in three of the HPLC runs, was at Val[141]-Thr[142]. The C-terminal fragments shown in Figure 6a had an N-terminal sequence consistent with this site. Three other cleavage sites, observed in only one run each, occurred after isoleucine at Ile[153]-Glu[154] and Ile[173]-Ser[174]; and after valine at Val[159]-Glu[160]. For three of the HPLC runs IGFBP-1 was degraded with the heparin-affinity eluate. A further cleavage site at Thr[132]-Tyr[133] was seen when urine was used, which probably represents cleavage by pepsin, or a pepsin-like protease [23].

Effect of IGFBP-1 cleavage on IGF binding. The interaction of proteolysed IGFBP-1 with IGF-I and IGF-II biosensor surfaces was analyzed (Biacore). In Figure 7 we show the biosensorgrams for the interaction of 200 nM

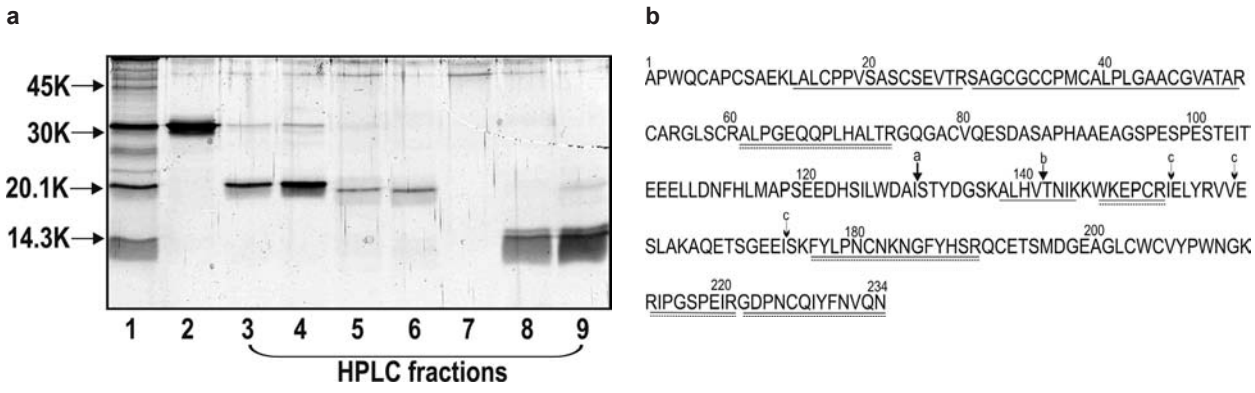

Figure 6. IGFBP-1 fragments generated by azurocidin-dependent proteolysis. (*a*) Recombinant npIGFBP-1 was incubated with (lane 1) and without (lane 2) 0.25 µl purified protease with an azurocidin:substrate ratio of 1:3500 for 2 h at 37 °C. The fragments were purified on HPLC. Lanes 3–6, purified fragments starting with the N-terminal sequence of IGFBP-1, starting APWQCAP-. Lane 7, fragment starting with the sequence STYDGSK-. Lanes 8, 9, purified C-terminal fragments starting with the sequence TNIKKWK-. Samples were separated on 12% SDS-PAGE and visualized by silver staining. Molecular mass markers are indicated by the arrows. (*b*) Summary of sequence analysis of IGFBP-1 fragments after proteolysis. N-terminal sequence analysis was performed on fragments purified by HPLC on four separate occasions. C-terminal sequence analysis was performed on one HPLC run. Cleavage sites are indicated by the arrows. a, the primary cleavage site present in four runs. b, a secondary cleavage site, present in three runs. c, cleavage sites, each identified in only one of the four runs. MALDI-MS analysis was performed on tryptic digests of fragments excised from SDS-PAGE. Continuous lines indicate sequences present in the approx. 20-kDa fragments. Broken lines indicate those in the 14-kDa forms.

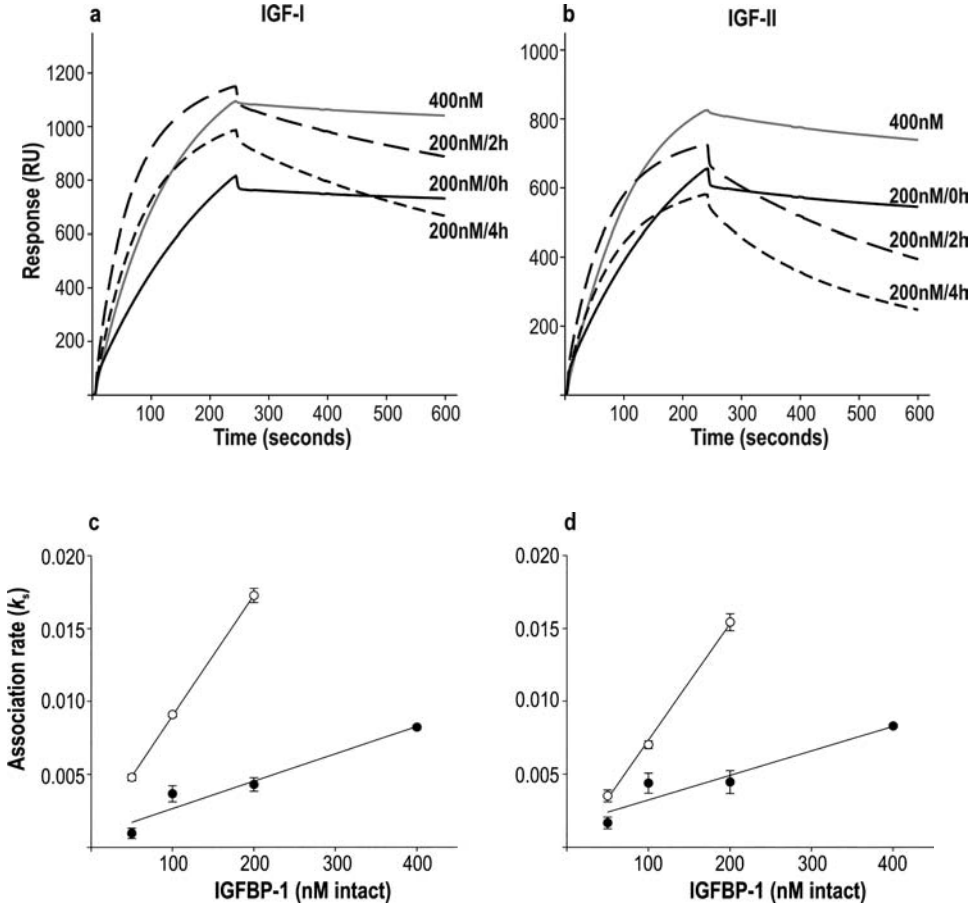

Figure 7. Biacore analysis of intact and proteolysed pIGFBP-1 over IGF-I and IGF-II biosensor surfaces. Recombinant pIGFBP-1 was analyzed across IGF-I (*a*, *c*) and IGF-II (*b*, *d*) biosensor surfaces. A concentration range of 50, 100, 200, 400 nM was analyzed at a flow rate of 10 µl/min. (*a*, *b*) Mean sensorgrams for 400 nM IGFBP-1 (intact, $n = 3$) and 200 nM IGFBP-1, intact (0 h, $n = 4$) and after 2-h ($n = 5$) and 4-h ($n = 3$) incubations with purified protease with an azurocidin:substrate ratio of 1:3500 for 2 h at 37 °C. (*c*, *d*) The rate of association (k_s), the absolute value of the slope (dRU/dt *versus* RU) over the linear initial association phase (21–120 s), is shown for pIGFBP-1, intact (closed circles), and after incubation with purified protease for 2 h at 37 °C (open circles).

Table 1. Kinetic analysis of interactions of intact and proteolysed pIGFBP-1 with IGF biosensor surfaces. The kinetic data shown in Figure 6 were analyzed using the 1:1 Langmuir interaction model. IGFBP-I was injected either intact, or after 2- or 4-h proteolysis, over IGF-I and IGF-II biosensor surfaces. The rates of association (over 21–120 s, k_s) and dissociation (over 261–360 s, k_d) are expressed as the mean ± SEM. The rates relative to that of 200 nM intact pIGFBP-1 and to that of IGF-I are also shown.

	IGFBP-1 (nM)	Proteolysis duration (h)	k_s ($\times 10^{-3}$ s^{-1})	Rel k_s	Rel to IGF-I	k_d ($\times 10^{-4}$ s^{-1})	Rel k_d	Rel to IGF-I
IGF-I								
	400	0	8.21 ± 0.14	1.91		1.45 ± 0.02	1.00	
	200	0	4.29 ± 0.46	1.00		1.46 ± 0.19	1.00	
	200	2	17.26 ± 0.49	4.02*		6.40 ± 0.25	4.40*	
	200	4	12.69 ± 0.08	2.96*†		11.36 ± 0.05	7.81*†	
IGF-II								
	400	0	8.30 ± 0.13	1.86	1.01	3.37 ± 0.02	0.97	2.33‡
	200	0	4.47 ± 0.78	1.00	1.02	3.48 ± 0.40	1.00	2.41‡
	200	2	15.43 ± 0.58	3.45*	0.89	15.99 ± 0.19	4.59*	2.51‡
	200	4	12.80 ± 0.08	2.86*†	1.01	27.17 ± 0.12	7.81*†	2.39‡

* $p < 0.001$, relative to 200 nM intact IGFBP-1.
† $p < 0.001$, relative to 200 nM IGFBP-1, proteolysed 2 h.
‡ $p < 0.001$, relative to IGF-I.

pIGFBP-1 intact, and after 2- and 4-h incubations with our partially purified protease, with immobilized IGF-I (Fig. 7a) and IGF-II (Fig. 7b). The kinetic analyses of the rates of association (over 21–120 s, k_s) and dissociation (over 261–360 s, k_d) for the results shown in Figure 7a and b are summarized in Table 1. Proteolysis of 200 nM IGFBP-1 for 2 h resulted in a greater than threefold increase in the rates of association and dissociation when analyzed across both IGF-I and IGF-II. The rate of dissociation further increased to more than sevenfold at the 4-h time point. The rate of dissociation of IGFBP-1 from IGF-II was greater than twice that from IGF-I, and proteolysis had no effect on this relationship. The apparent k_a was calculated from the slope of the association rate (k_s) and various concentrations of IGFBP-1 (Fig. 7c, d), and was $1.87 \pm 0.34 \times 10^4$ $M^{-1}s^{-1}$ for the interaction between IGFBP-1 and IGF-I and $1.68 \pm 0.38 \times 10^4$ $M^{-1}s^{-1}$ for the interaction between IGFBP-1 and IGF-II. The apparent k_a increased after proteolysis to $8.30 \pm 0.10 \times 10^4$ $M^{-1}s^{-1}$ for the interaction between 2-h proteolysed IGFBP-1 and IGF-I, and $8.01 \pm 0.35 \times 10^4$ $M^{-1}s^{-1}$ for IGF-II. However, there was also an increase in the maximum biosensor response for the IGF-I chip, suggesting an increase in the number of IGF-binding sites after proteolysis. At the 2-h time point of proteolysis, the predicted maximum response for interaction with IGF-I, based on the initial rate of association (21–120 s), was 1156 ± 16 RU, significantly greater than 908 ± 79 RU for intact IGFBP-1 ($p = 0.011$).

Biological effects of intact and proteolysed IGFBP-1. We studied the effect of pIGFBP-1 on IGF-II action in cultured cells. In the human breast cancer cell line MCF-7, 10 ng/ml IGF-II stimulated [^{3}H]thymidine incorporation 2-fold (range 1.5–2.7; six experiments, $p = 0.028$). Addition of 90 ng/ml intact pIGFBP-1 decreased this to 1.5-fold (range 1.2–2.1; six experiments, $p = 0.028$), whereas no inhibition was seen when proteolysed IGFBP-1 was added. In four of the experiments the effect of pIGFBP-1 alone was also determined, and resulted in a significant inhibition of [^{3}H]thymidine incorporation with intact pIGFBP-1 (range 13–33%, $p = 0.030$), and not with

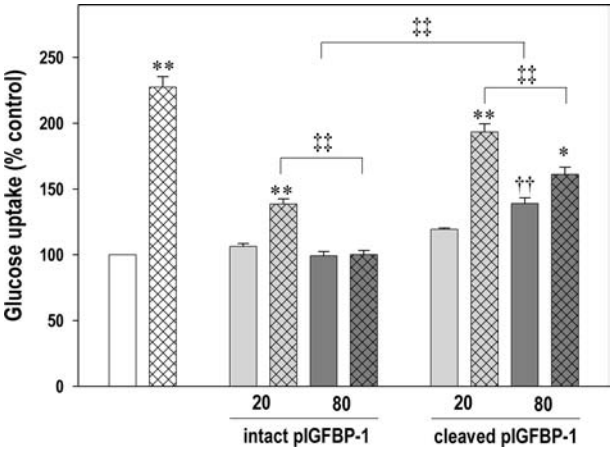

Figure 8. Effect of proteolysis on pIGFBP-1 action on glucose uptake into primary human skeletal myotube culture. Primary human skeletal myotubes were incubated under serum-free conditions for 24 h. Glucose uptake was determined as described in the Methods. The results are the mean ± SEM of four experiments using cells from different individuals each with three replicates; and are expressed as the percentage of uptake in the absence of IGF-II or IGFBP-1 for each. The effect of IGF-II is shown in the hatched bars. The effect of pIGFBP-1 on stimulation of glucose uptake by 10 ng/ml IGF-II was analyzed by two-way ANOVA for each of the 20 ng/ml and 80 ng/ml concentrations; * $p < 0.01$, ** $p < 0.001$, compared with no IGF-II; †† $p < 0.001$, compared with no IGFBP-1 or intact IGFBP-1. The effect of 20 ng/ml compared with 80 ng/ml IGFBP-1 on IGF-II-stimulated glucose uptake was compared in a separate two-way ANOVA; ‡‡ significant difference between intact and proteolysed IGFBP-1, and a significant effect of concentration; each $p < 0.001$, with no interaction.

proteolysed pIGFBP-1. We determined the effect of pIGFBP-1 on glucose uptake in primary human skeletal myoblasts after differentiation into myotubes (Fig. 8). A submaximal concentration of IGF-II, 10 ng/ml, stimulated glucose uptake more than 2-fold ($p < 0.001$) and was inhibited in a dose-response manner by both intact and proteolysed IGFBP-1. The inhibitory effect of the proteolytic fragments of IGFBP-1 was significantly less than that of intact IGFBP-1 ($p < 0.001$). Proteolysed IGFBP-1, in the absence of exogenous IGF-II, stimulated glucose uptake (80 ng/ml; $p < 0.001$), while intact pIGFBP-1 had no effect alone.

Identification of the neutral IGFBP-1 protease. HPLC purification confirmed the presence of azurocidin, myeloperoxidase and lactoferrin, but resulted in loss of proteolytic activity on IGFBP-1. Exposure of our heparin affinity-purified active material to 0.1% TFA in the HPLC buffer, followed by lyophilization and reconstitution in assay buffer abolished the IGFBP-1 proteolytic activity, as did reduction with dithiothreitol. A commercially available preparation of recombinant human azurocidin$^{27–250}$, produced in mouse myeloma cells, had no effect on IGFBP-1. Under reduced conditions, recombinant azurocidin migrated on SDS-PAGE at approximately 23 kDa, in contrast to the native material, which migrated at approximately 30 kDa (data not shown). Thus, the proteolytic activity, if related to azurocidin, is concluded to be a chemically modified form of azurocidin.

Although contamination by further proteins was estimated at less than 1% based on intact sequencer degradation and on peptide mass patterns, we considered the possibility that a very potent heparin-binding protease might be responsible for the activity. We showed that elastase, cathepsin G and proteinase 3, belonging to the same family as azurocidin, were all capable of degrading IGFBP-1. The activity of elastase was completely inhibited by the monoclonal antibody to azurocidin, while degradation by cathepsin G and proteinase 3, was partially inhibited (data not shown). There were clear differences, however, in the patterns of IGFBP-1 fragmentation. In Figure 4b we show the effect of elastase, which generated major fragments of 18 and 11 kDa, in contrast to the 22-, 20- and 14-kDa forms generated by our purified protease. There were also numerous minor fragments formed after incubation with elastase and not seen after incubation with azurocidin. Cathepsin G generated fragments of approximately 20 and 16 kDa, while proteinase 3 generated fragments of 26, 22, 20 and 16 kDa (data not shown). The proteolytic fragments generated by our protease were characterized by a high degree of stability. As the temperature of incubation was increased, there was further processing of the fragments by elastase (Fig. 4b).

Discussion

We have discovered a protease that is specific for IGFBP-1, and efficiently cleaves both the non-phosphorylated isoform and the phosphorylated form, with its high affinity for IGF-I [4]. Cleavage of pIGFBP-1 by this protease generated fragments that together have higher association and dissociation rates for IGFs compared with the intact protein. We also demonstrated a higher total capacity for IGF-I binding, suggesting that both and N- and C-terminal fragments may interact with ligand independently of each other. This would result in an increase in IGF turnover and availability to tissues. We have shown in human MCF-7 breast cancer cells and in human primary skeletal muscle cells that the inhibitory effect of pIGFBP-1 on IGF-II-stimulated DNA synthesis and glucose uptake is decreased after proteolysis.

IGFBP-1 is cleaved at a unique site by this novel protease activity. The P1 specificity was for isoleucine, and also valine, both of which are hydrophobic amino acids. The specificity of the cleavage site is consistent with predications for azurocidin activity, based on phage display selection of P1 mutants of aprotinin [24]. The primary site of cleavage was at Ile^{130}-Ser^{131}, in a region that is highly conserved in IGFBP-1 between species [7], and is not found in other IGFBPs [25]. The serine residue at the site has not been reported as significantly phosphorylated, whereas Ser^{101}, Ser^{119}, Ser^{169} are sites of phosphorylation that increase the affinity for IGF-I [26], and confer resistance to previously described proteases [13]. Cleavage generated a 130-amino acid N-terminal fragment that, when purified, migrated at 20 kDa on SDS-PAGE; and a 104-amino acid C-terminal fragment. Further cleavage at Val^{141}-Thr^{142} was often seen, generating a 93-amino acid fragment that, when purified, migrated at 14 kDa. When IGFBP-1 is cleaved and subjected to SDS-PAGE, and tryptic digests of the 20- and 14-kDa bands analyzed, sequences corresponding to both N- and C-terminal regions are detected. We speculate therefore that the C-terminal fragment may form dimers and that there is some further degradation of the N-terminal fragment. This is supported by the observation that 20- and 14-kDa bands are visible after cleaving IGFBP-1 that is biotinylated on the N terminus. Both of the C-terminal fragments that we have identified (IGFBP-1$^{131–234}$ and IGFBP-1$^{142–234}$) contain the RGD sequence of IGFBP-1 and are, therefore, expected to retain activity through interaction with the $\alpha_5\beta_1$ integrin receptor. A C-terminal fragment isolated from amniotic fluid starting at Val^{141}, is reported to have an IGF-independent effect on cell migration compared with intact IGFBP-1 [27]. Whether the effect on glucose uptake into human skeletal muscle cells by proteolysed IGFBP-1 alone could be attributed to an IGF-independent effect via the RGD sequence has to be elucidated in future studies.

We conclude that azurocidin is the specific IGFBP-1 protease based on (i) its presence in the partially purified active material, (ii) the inhibitory effect of a monoclonal antibody to azurocidin (iii) immunodepletion of active protease using this antibody, and (iv) clear differences in the pattern of fragmentation and stability of fragments compared with other candidate proteases. The recombinant azurocidin that is commercially available lacked activity on IGFBP-1 and had a lower molecular mass on SDS-PAGE, which is likely to be due to differences in *N*-glycosylation [28]. This glycosylation difference, or another post-translational difference likely accounts for the lack of protease activity. Alternatively, activity may have been lost during purification.

The fact that azurocidin may be a specific protease was unexpected. Although closely structurally related to three other neutrophil granule serprocidins, elastase, proteinase 3 and cathepsin G, azurocidin is generally regarded as proteolytically inactive due to loss of the catalytically active Ser^{175} [29–31]. However, human azurocidin has further residue differences at the active site compared to human elastase and proteinase 3, and has by additional replacements gained Ser^{41} as well as other residues towards other serprocidins, such that adjacent Ser and Asp residues still exist at the active site pocket, possibly supplying the necessary residues for catalytic proteolysis. Elastase and cathepsin G have been described to cleave IGFBP-1, but also degrade all of the IGFBPs, with IGFBP-5 and IGFBP-3 and -4, respectively, as preferred substrates [32]. We have shown that proteinase 3 can also cleave IGFBP-1. However, for each of these three proteases, there were clear differences in the patterns of fragmentation, and in the stability of the IGFBP-1 fragments compared with those generated by our protease. The stability of the IGFBP-1 fragments generated in the presence of azurocidin was remarkable, and contrasts to the effect of other proteases, with no further degradation seen after 24-h incubation at 37 °C or after a 2-h incubation at 45 °C.

Azurocidin is a multifunctional protein that is readily mobilized from secretory granules and is antimicrobial, chemotactic and induces cytokine secretion [33]. It therefore has an important role in host defense against inflammation and infection. The proteolytic effect on IGFBP-1 is noticeable at a nanomolar concentration of azurocidin in the purified preparation, substantially less than that required for other effects of azurocidin. For example, monocyte chemotaxis requires a micromolar concentration [34]. The optimal pH also differs. Its bactericidal action is maximal in the acidic conditions that are present in lysosomal granules, and this activity decreases by at least 50% when the pH is increased from 5.5 to 6.5 [30]. Its action on IGFBP-1, however, is greater above pH 6.

We isolated this IGFBP-1 protease from the urine of an individual with multiple myeloma and atopy, and succeeded in separating it from an acid-activated pepsin-like protease. We do not know the tissue source of the IGFBP-1 protease activity in this urine; however, it was co-purified with myeloperoxidase and lactoferrin, proteins that are also abundant in polymorphonuclear leukocytes [35]. The pathophysiological significance of IGFBP-1-specific proteolysis in an individual with multiple myeloma is yet to be clarified. To our knowledge expression of azurocidin has not been reported in any lymphoid lineage and it seems likely that inflammatory cells (neutrophils), which are associated with this malignancy, are the source. It appears possible that the presence of active azurocidin through IGFBP-1 proteolysis might increase myeloma cell growth and survival [14]. In addition to its expression in neutrophils, azurocidin is expressed in vascular endothelial cells in response to inflammatory mediators. Its expression is associated, for example, with atherosclerotic lesions [36].

IGFBP-1 and azurocidin both have important roles in inflammation and catabolism. IGFBP-1 increases dramatically in catabolic states, circulates in the phosphorylated isoform [37], accumulates in peripheral tissues, including skeletal muscle [38] and inhibits IGF-I action. Our finding that it can be degraded is therefore of considerable physiological and pharmacological interest. We conclude that the generation of IGF-binding fragments with lower IGF affinity will increase turnover and IGF availability in target tissues. Hence, a new factor in the regulation of IGF activity has been identified.

Acknowledgements. We are grateful to Olle Danielsson for helpful discussions and to the Persson Family Foundation and the Berth von Kantzow Foundation for financial support.

1 Firth, S. M. and Baxter, R. C. (2002) Cellular actions of the insulin-like growth factor binding proteins. Endocr. Rev. 23, 824–854.
2 Lewitt, M. S. (1994) Role of the insulin-like growth factors in the endocrine control of glucose homeostasis. Diab. Res. Clin. Pract. 23, 3–15.
3 Westwood, M., Gibson, J. M. and White, A. (1997) Purification and characterization of the insulin-like growth factor-binding protein-1 phosphoform found in normal plasma. Endocrinology 138, 1130–1136.
4 Jones, J. I., D'Ercole, A. J., Camacho-Hubner, C. and Clemmons, D. R. (1991) Phosphorylation of insulin-like growth factor (IGF)-binding protein 1 in cell culture and *in vivo*: Effects on affinity for IGF-I. Proc. Natl. Acad. Sci. USA 88, 7481–7485.
5 Lang, C. H., Nystrom, G. J. and Frost, R. A. (1999) Regulation of IGF binding protein-1 in Hep G2 cells by cytokines and reactive oxygen species. Am. J. Physiol. 276, G719–G727.
6 Lewitt, M. S. (2001) Stimulation of IGF-binding protein-1 secretion by AMP-activated protein kinase. Biochem. Biophys. Res. Commun. 282, 1126–1131.
7 Lee, P. D. K., Giudice, L. C., Conover, C. A. and Powell, D. R. (1997) Insulin-like growth factor binding protein-1: recent findings and new directions. Proc. Soc. Exp. Biol. Med. 216, 319–357.
8 Mesotten, D., Delhanty, P. J., Vanderhoydonc, F., Hardman, K. V., Weekers, F., Baxter, R. C. and Van den Berghe, G. (2002) Regulation of insulin-like growth factor binding protein-1 dur-

ing protracted critical illness. J. Clin. Endocrinol. Metab. 87, 5516–5523.
9 de Groof, F., Joosten, K. F., Janssen, J. A., de Kleijn, E. D., Hazelzet, J. A., Hop, W. C., Uitterlinden, P., van Doorn, J. and Hokken-Koelega, A. C. (2002) Acute stress response in children with meningococcal sepsis: important differences in the growth hormone/insulin-like growth factor I axis between nonsurvivors and survivors. J. Clin. Endocrinol. Metab. 87, 3118–3124.
10 Frost, R. A. and Lang, C. H. (1999) Differential effects of insulin-like growth factor I (IGF-I) and IGF-binding protein-1 on protein metabolism in human skeletal muscle cells. Endocrinology 140, 3962–3970.
11 Póvoa, G., Enberg, G., Jörnvall, H. and Hall, K. (1984) Isolation and characterization of a somatomedin-binding protein from mid-term human amniotic fluid. Eur. J. Biochem. 144, 199–204.
12 Clay Bunn, R. and Fowlkes, J. L. (2003) Insulin-like growth factor binding protein proteolysis. Trends Endocrinol. Metab. 14, 176–181.
13 Gibson, J. M., Aplin, J. D., White, A. and Westwood, M. (2001) Regulation of IGF bioavailability in pregnancy. Mol. Hum. Reprod. 7, 79–87.
14 Kuehl, W. M. and Bergsagel, P. L. (2002) Multiple myeloma: evolving genetic events and host interactions. Nat. Rev. Cancer 2, 175–187.
15 Bayes-Genis, A., Conover, C. A. and Schwartz, R. S. (2000) The insulin-like growth factor axis: A review of atherosclerosis and restenosis. Circ. Res. 86, 125–130.
16 Jones, J. I., Gockerman, A., Busby, W. H., Wright, G. and Clemmons, D. R. (1993) Insulin-like growth factor binding protein-1 stimulates cell migration and binds to the $\alpha_5\beta_1$ integrin by means of its Arg-Gly-Asp sequence. Proc. Natl. Acad. Sci. USA 90, 10553–10557.
17 Bayes-Genis, A., Conover, C. A., Overgaard, M. T., Bailey, K. R., Christiansen, M., Holmes, D. R. Jr, Virmani, R., Oxvig, C. and Schwartz, R. S. (2001) Pregnancy-associated plasma protein A as a marker of acute coronary syndromes. N. Engl. J. Med. 345, 1022–1029.
18 Norin, A., Shafqat, J., El-Ahmad, M., Alvelius, G., Cederlund, E., Hjelmqvist, L. and Jörnvall, H. (2004) Class III alcohol dehydrogenase: consistent pattern complemented with the mushroom enzyme. FEBS Lett. 559, 27–32.
19 Roblick, U. J., Hirschberg, D., Habermann, J. K., Palmberg, C., Becker, S., Kruger, S., Gustafsson, M., Bruch, H. P., Franzen, B., Ried, T., Bergmann, T., Auer, G. and Jörnvall, H. (2004) Sequential proteome alterations during genesis and progression of colon cancer. Cell. Mol. Life Sci. 61, 1246–1255.
20 Bouzakri, K., Roques, M., Gual, P., Espinosa, S., Guebre-Egziabher, F., Riou, J. P., Laville, M., Le Marchand-Brustel, Y., Tanti, J. F. and Vidal, H. (2003) Reduced activation of phosphatidylinositol-3 kinase and increased serine 636 phosphorylation of insulin receptor substrate-1 in primary culture of skeletal muscle cells from patients with type 2 diabetes. Diabetes 52, 1319–1325.
21 Bouzakri, K., Roques, M., Debard, C., Berbe, V., Rieusset, J., Laville, M. and Vidal, H. (2004) WY-14643 and 9- cis-retinoic acid induce IRS-2/PI 3-kinase signalling pathway and increase glucose transport in human skeletal muscle cells: differential effect in myotubes from healthy subjects and Type 2 diabetic patients. Diabetologia 47, 1314–1323.
22 Tanaka, T. and Yada, R. Y. (2001) N-terminal portion acts as an initiator of the inactivation of pepsin at neutral pH. Protein Eng. 14, 669–674.
23 Luthman, H., Söderling-Barros, J., Persson, B., Engberg, C., Stern, I., Lake, M., Franzén, S.-Å., Israelsson, M., Råden, B., Lindgren, B., Hjelmqvist, L., Enerbäck, S., Carlsson, P., Bjursell, G., Póvoa, G., Hall, K. and Jörnvall, H. (1989) Human insulin-like growth-factor-binding protein. Low-molecular-mass form: protein sequence and cDNA cloning. Eur. J. Biochem. 180, 259–265.
24 Kiczak, L., Koscielska, K., Otlewski, J., Czerwinski, M. and Dadlez, M. (1999) Phage display selection of P1 mutants of BPTI directed against five different serine proteinases. Biol. Chem. 380, 101–105.
25 Hwa, V., Oh, Y. and Rosenfeld, R. G. (1999) The insulin-like growth factor-binding protein (IGFBP) superfamily. Endocr. Rev. 20, 761–787.
26 Jones, J. I., Busby, W. H., Wright, G., Smith, C. E., Kimack, N. M. and Clemmons, D. R. (1993) Identification of the sites of phosphorylation in insulin-like growth factor binding protein-1. Regulation of its affinity by phosphorylation of serine 101. J. Biol. Chem. 268, 1125–1131.
27 Sala, A., Capaldi, S., Campagnoli, M., Faggion, B., Labo, S., Perduca, M., Romano, A., Carrizo, M. E., Valli, M., Visai, L., Minchiotti, L., Galliano, M. and Monaco, H. L. (2005) Structure and properties of the C-terminal domain of insulin-like growth factor binding protein-1 isolated from human amniotic fluid. J. Biol. Chem. 280, 29812–29819.
28 Olczak, M. and Watorek, W. (2002) Structural analysis of N-glycans from human neutrophil azurocidin. Biochem. Biophys. Res. Commun. 293, 213–219.
29 Wilde, C. G., Snable, J. L., Griffith, J. E. and Scott, R. W. (1990) Characterization of two azurophil granule proteases with active-site homology to neutrophil elastase. J. Biol. Chem. 265, 2038–2041.
30 Campanelli, D., Detmers, P. A., Nathan, C. F. and Gabay, J. E. (1990) Azurocidin and a homologous serine protease from neutrophils. Differential antimicrobial and proteolytic properties. J. Clin. Invest. 85, 904–915.
31 Pereira, H. A., Spitznagel, J. K., Pohl, J., Wilson, D. E., Morgan, J., Palings, I. and Larrick, J. W. (1990) CAP 37, a 37 kDa human neutrophil granule cationic protein shares homology with inflammatory proteinases. Life Sci. 46, 189–196.
32 Gibson, T. L. B. and Cohen, P. (1999) Inflammation-related neutrophil proteases, cathepsin G and elastase, function as insulin-like growth factor binding protein proteases. Growth Horm. IGF Res. 9, 241–253.
33 Watorek, W. (2003) Azurocidin: inactive serine proteinase homolog acting as a multifunctional inflammatory mediator. Acta Biochim. Pol. 50, 743–752.
34 Okuyama, Y., Cho, J. H., Nakajima, Y., Homma, K., Sekimizu, K. and Natori, S. (2004) Binding between azurocidin and calreticulin: its involvement in the activation of peripheral monocytes. J. Biochem. (Tokyo) 135, 171–177.
35 Borregaard, N. and Cowland, J. B. (1997) Granules of the human neutrophilic polymorphonuclear leukocyte. Blood 89, 3503–3521.
36 Lee, T. D., Gonzalez, M. L., Kumar, P., Chary-Reddy, S., Grammas, P. and Pereira, H. A. (2002) CAP37, a novel inflammatory mediator: its expression in endothelial cells and localization to atherosclerotic lesions. Am. J. Pathol. 160, 841–848.
37 Frost, R. A., Bereket, A., Wilson, T. A., Wojnar, M. M., Lang, C. H. and Gelato, M. C. (1994) Phosphorylation of insulin-like growth factor binding protein-1 in patients with insulin-dependent diabetes mellitus and severe trauma. J. Clin. Endocrinol. Metab. 78, 1533–1535.
38 Fan, J., Molina, P. E., Gelato, M. C. and Lang, C. H. (1994) Differential tissue regulation of insulin-like growth factor-I content and binding proteins after endotoxin. Endocrinology 134, 1685–1692.